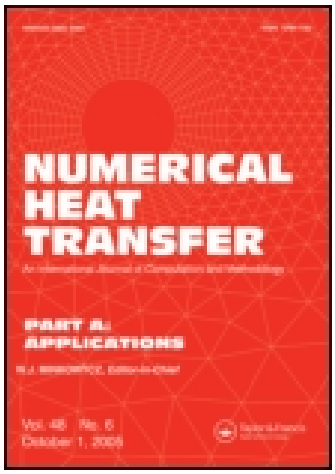

Numerical Heat Transfer, Part A: Applications: An International Journal of Computation and Methodology
Publication details, including instructions for authors and subscription information:
http://www.tandfonline.com/loi/unht20

NUMERICAL TREATMENT OF DIFFUSION COEFFICIENTS AT INTERFACES

K. C. Chang [a] & U. J. Payne [a]
[a] Institute of Aeronautics and Astronautics, National Cheng-Kung University , Tainan, Taiwan, 70101, Republic of China
Published online: 13 Jul 2010.

To cite this article: K. C. Chang & U. J. Payne (1992) NUMERICAL TREATMENT OF DIFFUSION COEFFICIENTS AT INTERFACES, Numerical Heat Transfer, Part A: Applications: An International Journal of Computation and Methodology, 21:3, 363-376, DOI: 10.1080/10407789208944882

To link to this article: http://dx.doi.org/10.1080/10407789208944882

Numerical Heat Transfer, Part A, vol. 21, pp. 363–376, 1992

NUMERICAL TREATMENT OF DIFFUSION COEFFICIENTS AT INTERFACES

K. C. Chang and U. J. Payne
Institute of Aeronautics and Astronautics, National Cheng-Kung University, Tainan 70101, Taiwan, Republic of China

The main purpose of this work is to evaluate the values of diffusion coefficients at control-volume faces, using the finite-volume method, in transport problems that include diffusion processes. A heat conduction problem in a composite slab with linearly temperature-dependent conductivity, which has a closed-form solution, is selected for demonstration. It is found that the harmonic mean operation performs better than the arithmetic mean operation in evaluating the interface diffusion coefficients. Moreover, if we intend to obtain the information at some specific interfaces with abrupt changes of diffusion coefficients, the recommended grid layout is arranged such that each specific interface contains a grid node. This arrangement can give more accurate predictions at these unusual interfaces.

INTRODUCTION

The transport equations that govern fluid flow, heat transfer, mass transfer, and other related processes are usually cast into a general form consisting of unsteady, convection, diffusion, and source terms, as follows:

$$\frac{\partial}{\partial t}(\rho\phi) + \text{div}\,(\rho\mathbf{u}\phi) = \text{div}\,(\Gamma\,\text{grad}\,\phi) + S \tag{1}$$

where Γ is the diffusion coefficient and ϕ represents a dependent variable. Equation (1) is a nonlinear partial differential equation, and there is little hope of solving this kind of equation analytically. Many numerical methods are applicable to obtain the solution of Eq. (1). Among them, the finite-volume method, which adopts the control-volume formulation and lends itself to conservation laws, is widely used in thermal fluid problems and is discussed in detail here.

The basic idea of the discretization procedure of Eq. (1) is as follows. The calculation domain is divided into a number of nonoverlapping control volumes such that there is one control volume surrounding each grid node. Equation (1) is integrated over each control volume; the result is a discretization equation containing the values of ϕ for a group of grid nodes. Since the gradient of ϕ in the diffusion term is evaluated from the piecewise-linear profile [1], the diffusion coefficient must be the value pertaining to the interface of two neighboring control volumes. Unless the diffusion coefficient is uniformly distributed in the entire computational domain, a situation that is not usually encountered in practical engineering problems, a prescription is needed for evaluating

NOMENCLATURE

a	coefficient in discretization equation	ρ	density
f	interpolation factor	ϕ	dependent variable
q	heat flux	**Subscripts**	
S	source term		
t	time	i	interface
T	temperature	i, j	node indices
$\mathbf{u}$	velocity vector	L	boundary on the right-hand side
U	transformed temperature	m	material index
w	slab width	n	series index
x, y	coordinates	O	boundary on the left-hand side
α	linearly dependent temperature constants	$+, -$	right- and left-hand sides of interface
β	eigenvalue	0	reference temperature
Γ	diffusion coefficient	1, 2	materials 1 and 2
δ	distance between adjacent nodes	**Superscript**	
Δ	control-volume length		
λ	thermal conductivity	(m)	material index

the interface diffusion coefficient in terms of the grid-node values. This is the principal objective to be studied in this work.

There are two types of grid arrangements that are applicable to incompressible flow problems. One is the nonstaggered grid, in which all dependent variables are located at the same grid nodes. The other is the staggered grid [2], which is used for resolving the pressure-velocity coupling in the Navier-Stokes equations. In the staggered grid, the velocity components are located at the nodes that lie on the faces of the control volumes. The effective viscosities at all interfaces can be directly evaluated from the values of dependent variables at the normal grid nodes without special treatment. For heat and mass transfer, however, the problem is still present, even in the staggered grid.

The most straightforward procedure to obtain the interface diffusion coefficient is to linearly interpolate from two neighboring nodes. Another popular procedure is to take the harmonic mean value of the two diffusion coefficients at the neighboring nodes, which represents the exact solution for a steady, one-dimensional diffusion-type problem (without a source). The operation of the harmonic mean is given in Eq. (15*a*). Patankar studied a conduction problem in composite material and recommended the harmonic mean operation rather than the arithmetic mean operation for evaluating the interface diffusion coefficient [3]. In this work, we attempt to reexamine these two extensively used mean operations in evaluating interface thermal conductivity for a nonlinear heat conduction problem, and then suggest an alternative grid arrangement to avoid the approximation errors. Finally, we extend our application to general transport problems that exhibit a variation of diffusion coefficients in their computational domains.

EXAMPLE PROBLEM

Since we are interested in the numerical treatment of the diffusion term in Eq. (1), let us choose a diffusion-type problem that can be solved in closed form. Consider a two-dimensional rectangular slab with no energy generation, constructed of two differ-

ent materials, attached to bases of the same material, and held at two constant base temperatures. The slab is convection cooled at a constant temperature, and radiation with the air as well as the base surfaces can be disregarded if temperatures are not too high. Taking the environmental temperature as the reference temperature and using the symmetry characteristic, the example problem is shown schematically in Fig. 1. The dependence of thermal conductivity on temperature is assumed in the linear form:

$$\lambda_m = \lambda_{m0}(1 + \alpha_m T) \qquad m = 1, 2 \tag{2}$$

where λ_{m0} is the thermal conductivity of material m at the reference temperature and α_m is constant. The heat-conduction equations are formulated as follows:

$$\frac{\partial}{\partial x}\left[\lambda_1(T_1)\frac{\partial T_1}{\partial x}\right] + \frac{\partial}{\partial y}\left[\lambda_1(T_1)\frac{\partial T_1}{\partial y}\right] = 0 \qquad 0 < x < \frac{1}{2} \qquad 0 < y < w \tag{3a}$$

$$\frac{\partial}{\partial x}\left[\lambda_2(T_2)\frac{\partial T_2}{\partial x}\right] + \frac{\partial}{\partial y}\left[\lambda_2(T_2)\frac{\partial T_2}{\partial y}\right] = 0 \qquad 0 < x < \frac{1}{2} \qquad 0 < y < w \tag{3b}$$

$$T_1 = T_2 \qquad \text{at} \quad x = \frac{1}{2} \qquad 0 < y < w \tag{3c}$$

$$\lambda_1 \frac{\partial T_1}{\partial x} = \lambda_2 \frac{\partial T_2}{\partial x} \qquad \text{at} \quad x = \frac{1}{2} \qquad 0 < y < w \tag{3d}$$

The other associated boundary conditions are depicted in Fig. 1.

These nonlinear heat-conduction equations have been solved analytically, using the Kirchhoff transformation and the method of separation of variables [4]. The closed-form solution is expressed as

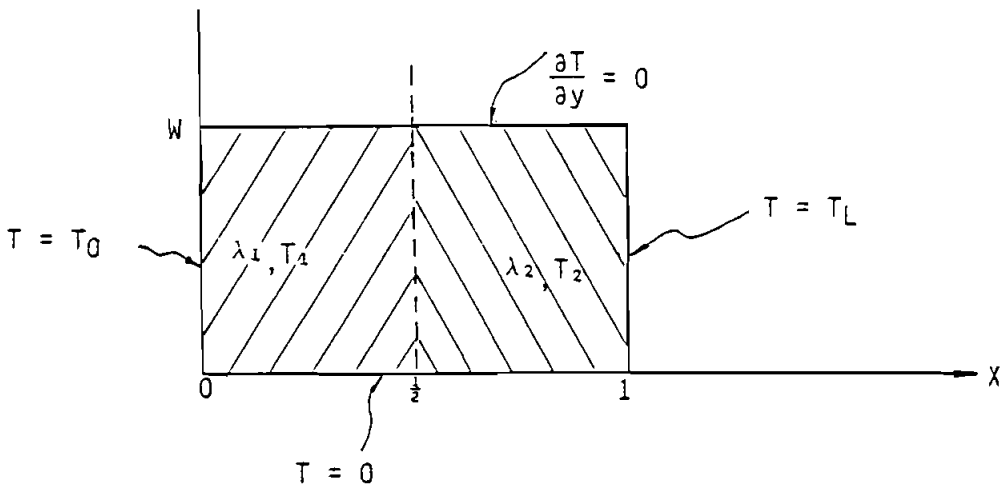

Fig. 1 Description of a composite slab.

$$U_1(x, y) = \sum_{n=0}^{\infty} \frac{\sin \beta_n y}{\sin h(\beta_n/2)} \left\{ \frac{2U_0}{w\beta_n} \sin h\left[\beta_n\left(\frac{1}{2} - x\right)\right] + (U_{i1})_n \sin h\beta_n x \right\} \tag{4a}$$

$$0 \le x \le \frac{1}{2} \qquad 0 \le y \le w$$

$$U_2(x, y) = \sum_{n=0}^{\infty} \frac{\sin \beta_n y}{\sin h(\beta_n/2)} \left\{ (U_{i2})_n \sin h[\beta_n(1 - x)] + \frac{2U_L}{w\beta_n} \sin h\left[\beta_n\left(x - \frac{1}{2}\right)\right] \right\} \tag{4b}$$

$$\frac{1}{2} \le x \le 1 \qquad 0 \le y \le w$$

where the eigenvalues are given by

$$\beta_n = \left(\frac{2n + 1}{2}\right)\frac{\pi}{\omega} \qquad n = 0, 1, 2, \ldots \tag{5}$$

and the two transformed boundary values are given by

$$U_0 = T_0 + \frac{\alpha_1}{2} T_0^2 \tag{6}$$

$$U_L = T_L + \frac{\alpha_2}{2} T_L^2 \tag{7}$$

The values of $(U_{i1})_n$ and $(U_{i2})_n$ are determined from the interfacial condition, Eq. (3c), as follows:

$$(U_{im})_n = T_{in} + \frac{\alpha_m w}{4} \beta_n T_{in}^2 \qquad m = 1, 2 \tag{8}$$

where

$$T_{in} = \frac{2}{w\beta_n(\lambda_{10}\alpha_1 + \lambda_{20}\alpha_2)} \left\{ \left[(\lambda_{10} + \lambda_{20})^2 + \frac{2}{\cos h(\beta_n/2)} \times (\lambda_{10}U_0 + \lambda_{20}U_L)(\lambda_{10}\alpha_1 + \lambda_{20}\alpha_2) \right]^{1/2} - (\lambda_{10} + \lambda_{20}) \right\} \tag{9}$$

The inverse transformation of $T(x, y)$ is given by

$$T_m(x, y) = \frac{1}{\alpha_m} [\sqrt{1 + 2\alpha_m U_m(x, y)} - 1] \qquad m = 1, 2 \tag{10}$$

If the thermal conductivities are independent of temperature, that is, $\alpha_1 = \alpha_2 = 0$, the closed-form solution can be obtained without transformation and expressed as

$$T_1(x, y) = \sum_{n=0}^{\infty} \frac{\sin \beta_n y}{\sin h(\beta_n/2)} \left\{ \frac{2T_O}{w\beta_n} \sin h\left[\beta_n\left(\frac{1}{2} - x\right)\right] + T_{in} \sin h\beta_n x \right\} \tag{11a}$$

$$0 \le x \le \frac{1}{2} \qquad 0 \le y \le w$$

$$T_2(x, y) = \sum_{n=0}^{\infty} \frac{\sin \beta_n y}{\sin h(\beta_n/2)} \left\{ T_{in} \sin h[\beta_n(1 - x)] + \frac{2T_L}{w\beta_n} \sin h\left[\beta_n\left(x - \frac{1}{2}\right)\right] \right\} \tag{11b}$$

$$\frac{1}{2} \le x \le 0 \qquad 0 \le y \le w$$

where T_{in} is now given in the following expression instead of Eq. (9):

$$T_{in} = \frac{2(\lambda_1 T_O + \lambda_2 T_L)}{w\beta_n(\lambda_1 + \lambda_2) \cos h(\beta_n/2)} \tag{12}$$

NUMERICAL ANALYSIS

Let us construct the control volume by placing the control-volume face midway between two neighboring grid nodes. The grid nodes are arranged so that the interface coincides with one of the control-volume faces, as shown in Fig. 2, and this grid arrangement is called grid system A. Each individual control volume is composed of homogeneous material. Consider that the control volume surrounding the grid node (i, j) is made of a material associated with the λ_1 conductivity, and the one around $(i + 1, j)$ is made of a material associated with the λ_2 conductivity. The discretization equation is obtained by integrating Eq. (3) over the control volume as follows:

$$q_{i+1/2,j}\,\Delta y_{i,j} - q_{i-1/2,j}\,\Delta y_{i,j} + q_{i,j+1/2}\,\Delta x_{i,j} - q_{i,j-1/2}\,\Delta x_{i,j} = 0 \tag{13}$$

where q denotes the heat flux across the control-volume face as depicted in Fig. 2. The heat flux that does not cross the interface is defined by

$$q^{(m)} = -\lambda_m \frac{\partial T}{\partial n} \qquad m = 1, 2 \tag{14}$$

where n is the unit length normal to the control-volume face. For the heat flux across the interface, the interface conductivity can be evaluated by either the harmonic mean or the arithmetic mean of the two conductivities of grid nodes (i, j) and $(i + 1, j)$, as expressed in the following:

$$\lambda_{i+1/2,j} = \frac{2\lambda_{i,j}\lambda_{i+1,j}}{\lambda_{i,j} + \lambda_{i+1,j}} \tag{15a}$$

or

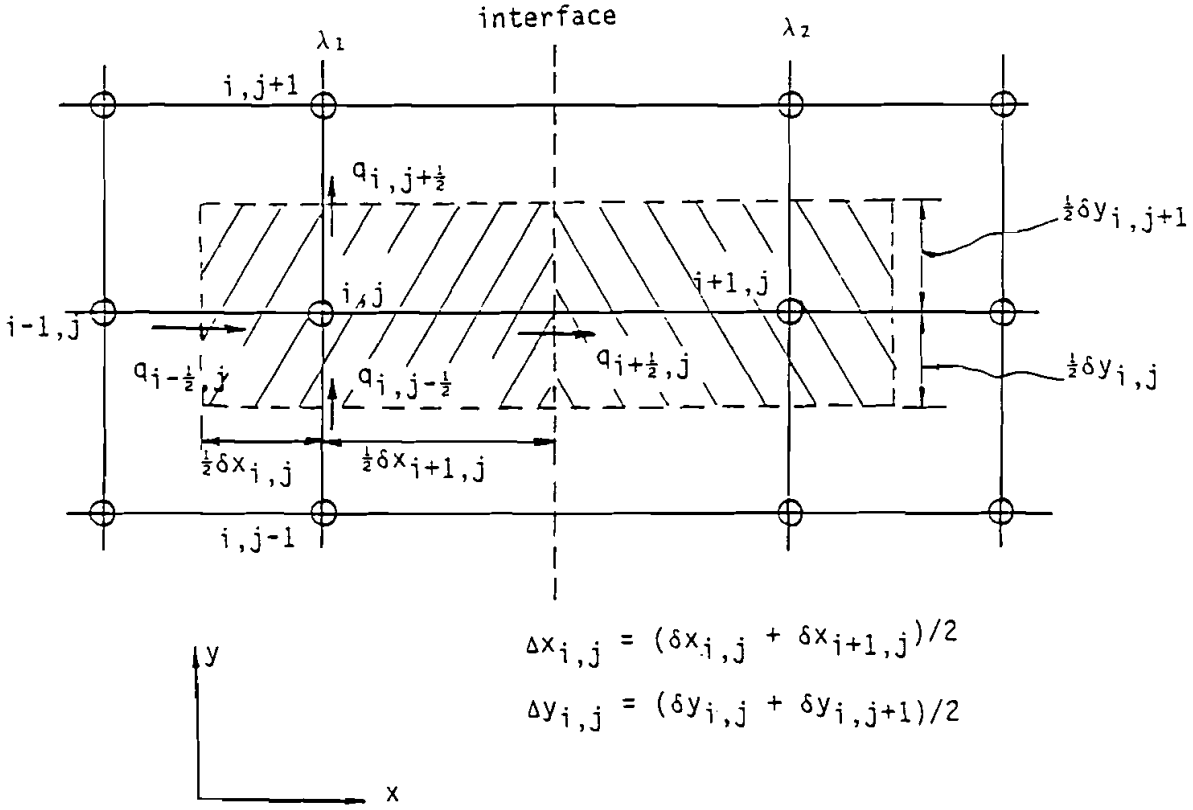

Fig. 2 Grid arrangement at the interface of grid system A.

$$\lambda_{i+1/2,j} = \frac{\lambda_{i,j} + \lambda_{i+1,j}}{2} \tag{15b}$$

Note that these two equations are essentially the same if $\lambda_{i,j} = \lambda_{i+1,j}$. Substitution of Eqs. (14) and (15) into Eq. (13) and employment of the piecewise-linear profile to calculate the derivatives yields

$$a_{i,j}T_{i,j} = a_{i-1,j}T_{i-1,j} + a_{i+1,j}T_{i+1,j} + a_{i,j-1}T_{i,j-1} + a_{i,j+1}T_{i,j+1} \tag{16a}$$

where

$$a_{i-1,j} = \lambda_1 \frac{\Delta y_{i,j}}{\delta x_{i,j}} \tag{16b}$$

$$a_{i+1,j} = \frac{2\lambda_1\lambda_2}{\lambda_1 + \lambda_2} \frac{\Delta y_{i,j}}{\delta x_{i+1,j}} \quad \text{for harmonic mean}$$

$$a_{i+1,j} = \frac{\lambda_1 + \lambda_2}{2} \frac{\Delta y_{i,j}}{\delta x_{i+1,j}} \quad \text{for arithmetic mean} \tag{16c}$$

$$a_{i,j-1} = \lambda_1 \frac{\Delta x_{i,j}}{\delta y_{i,j}} \tag{16d}$$

$$a_{i,j+1} = \lambda_1 \frac{\Delta x_{i,j}}{\delta y_{i,j+1}} \tag{16e}$$

$$a_{i,j} = a_{i-1,j} + a_{i+1,j} + a_{i,j-1} + a_{i,j+1} \tag{16f}$$

Similarly, the discretization equation for grid node $(i + 1, j)$ can be formulated in the form of Eq. (16), except that λ_1 and λ_2 are exchanged because the control volume is now made of material 2. This implies that, in terms of grid system A, the derivative $\partial T/\partial x$ at the left-hand side of the interface (material 1) is the same as that at the right-hand side (material 2). In other words, the first derivative of temperature with respect to an x-independent variable is continuous at the interface. However, as shown in Eq. (3*d*), $\partial T/\partial x$ must be discontinuous at the interface because $\lambda_1 \neq \lambda_2$. The jump condition of $\partial T/\partial x$ at the interface has been smoothed out in grid system A.

An alternative grid arrangement, called grid system B, is suggested in the following. One of the grid nodes, say (i, j), is located at the interface, as illustrated in Fig. 3. The control volume of the grid node (i, j) is then composed of two materials. According to the basic discretization concept of a continuous function, both materials 1 and 2, which lie in the control volume of (i, j), have the same values of $\partial T/\partial y$ at the faces of $(i, j - 1/2)$ and $(i, j + 1/2)$. The resultant heat flow at either control-volume face normal to the interface can be written as

$$q\,\Delta x_{i,j} = q^{(1)} \frac{\delta x_{i,j}}{2} + q^{(2)} \frac{\delta x_{i+1,j}}{2} \tag{17}$$

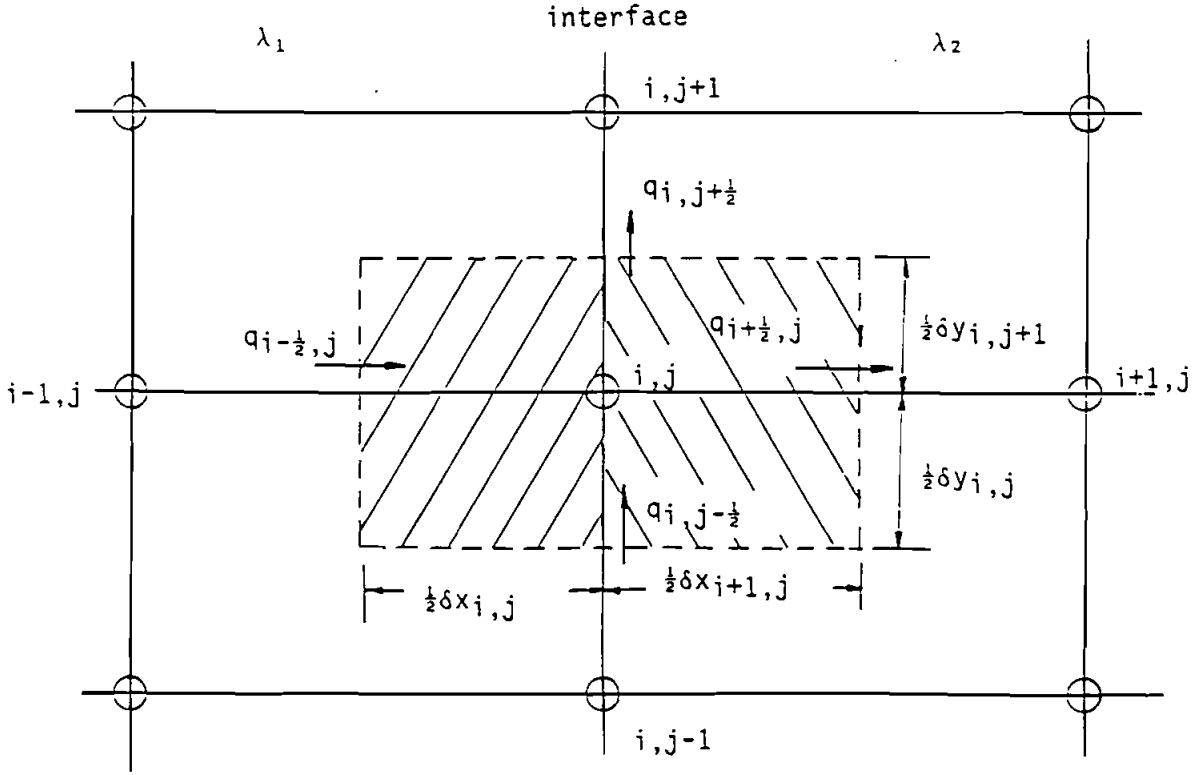

Fig. 3 Grid arrangement at the interface of grid system B.

Substitution of Eq. (14) into Eq. (17) gives

$$q = -[f\lambda_1 + (1 - f)\lambda_2] \frac{\partial T}{\partial y} \tag{18}$$

where the interpolation factor f is the volumetric ratio of composite constituents defined by

$$f = \frac{\delta x_{i,j}}{2\,\Delta x_{i,j}} \tag{19}$$

The conductivity for the control-volume face normal to the interface is thus determined by the arithmetic mean:

$$\lambda = f\lambda_1 + (1 - f)\lambda_2 \tag{20}$$

The discretization equation for the control volume of grid node (i, j) can now be written similar to the expression of Eq. (16), but where

$$a_{i+1,j} = \lambda_2 \frac{\Delta y_{i,j}}{\delta x_{i+1,j}} \tag{21a}$$

$$a_{i,j-1} = [f\lambda_1 + (1 - f)\lambda_2] \frac{\Delta x_{i,j}}{\delta y_{i,j}} \tag{21b}$$

$$a_{i,j+1} = [f\lambda_1 + (1 - f)\lambda_2] \frac{\Delta x_{i,j}}{\delta y_{i,j+1}} \tag{21c}$$

Note that this alternative numerical treatment does not violate the required interfacial boundary conditions, Eqs. (3*c*) and (3*d*), and does preserve the conservation principle of control-volume formulation. Furthermore, although we derive two-dimensional forms in the present work, the formulations for both grid systems are easy to extend to three-dimensional problems.

RESULTS AND DISCUSSION

Numerical experiments reveal that the grid layouts of 42 × 21 and 41 × 21 uniformly distributed nodes for grid systems A and B, respectively, have generated nearly grid-independent solutions for the example problem. In order to discriminate the differences in the solutions obtained with the different numerical treatments discussed in this work, we use a low gridline concentration in the following numerical study, that is, 22 × 11 and 21 × 11 uniformly distributed nodes for grid systems A and B, respectively.

There are two step functions of y in the example problem:

At $x = 0$

$$T = \begin{cases} 0 & y = 0 \\ T_O & 0 < y < w \end{cases} \tag{22a}$$

At $x = 1$

$$T = \begin{cases} 0 & y = 0 \\ T_L & 0 < y < w \end{cases} \tag{22b}$$

The closed-form solutions, which are in the form of a Fourier series, may have overshoots due to the Gibbs phenomenon at these two singular points [5]. The overshoots may be highly unreliable for precise solutions, particularly in the vicinity of the singular points. It was shown [4] that, as far as the grid layouts used in this work were concerned, the analytical solutions at the grid nodes could be free from the Gibbs phenomenon by inclusion of more terms (say, 30 terms) in the summation of the Fourier series shown in Eqs. (4) and (11).

Test Problem 1: Heat Conduction with One Abrupt Change of Temperature-Independent Conductivity

The calculation conditions are $T_O = 600$, $T_L = 100$, $w = 0.5$, $\lambda_{10} = 0.06$, $\lambda_{20} = 0.001$, and $\alpha_{10} = \alpha_{20} = 0$. Three numerical treatments are tested.

Case 1: Grid system A (see Fig. 2) with the harmonic mean conductivity at the interface.
Case 2: Same as case 1 but with conductivity of the arithmetic mean instead of the harmonic mean at the interface.
Case 3: Grid system B (see Fig. 3).

Figure 4 compares the relative errors produced by the three numerical treatments at three y positions. The relative errors are defined by

$$\text{error}\% = (\text{numerical solution/analytical solution} - 1) \times 100\% \tag{23}$$

It is seen in Fig. 4 that errors arise quickly as the node locations move to the singular points, (0, 0) and (1, 0). This occurrence is primarily attributed to the result of approximating the discretization. Within each control volume constructed by a grid node, the physical properties, such as temperature, are assumed to be uniformly distributed. When the grid nodes move close to the singular points, this assumption becomes ambiguous. The difficulty can be alleviated by placing more grid nodes around the singular points, but we cannot completely remove these approximation errors from the numerical solutions due to the existence of singularity. However, this kind of error can be overlooked if we focus our attention on the regions far away from the singular points. A comparison reveals that both cases 1 and 3 exhibit nearly the same prediction accuracies, whereas case 2 yields relatively higher prediction errors. This same observation was also made by Patankar [3]. The minor differences between cases 1 and 3 stem mainly from the different grid-node numbers used in grid systems A and B (as mentioned above, we

purposely use the low gridline concentration for demonstration). The conductivity at the interface determined in case 2 is 3.05×10^{-2} (the arithmetic mean), which is much larger than the harmonic mean value (1.97×10^{-3}) determined in case 1. The inappropriate evaluation of interface conductivity in case 2 results in larger errors in predictions, as shown in Fig. 4.

To further investigate the merits of cases 1 and 3, the determination of properties at the interface is discussed below.

Interpolation of the interface temperature in grid system A. Since the interface is placed midway between grid nodes (i, j) and $(i + 1, j)$, as illustrated in Fig. 2, the interface temperature $T_{i+1/2,j}$ can be interpolated from the convergent numerical solutions at these two neighboring nodes as follows:

$$\lambda_1 \left.\frac{\partial T}{\partial x}\right|_- = \lambda_2 \left.\frac{\partial T}{\partial x}\right|_+ = \frac{2\lambda_1\lambda_2}{\lambda_1 + \lambda_2} \left.\frac{\partial T}{\partial x}\right|_{i+1/2,j} \tag{24}$$

where the negative and positive subscripts denote the two neighboring sides of the interface, and

$$\left.\frac{\partial T}{\partial x}\right|_- = \frac{2(T_{i+1/2,j} - T_{i,j})}{\delta x_{i+1,j}} \tag{25}$$

$$\left.\frac{\partial T}{\partial x}\right|_{i+1/2,j} = \frac{T_{i+1,j} - T_{i,j}}{\delta x_{i+1,j}} \tag{26}$$

substitution of Eqs. (25) and (26) into Eq. (24) yields

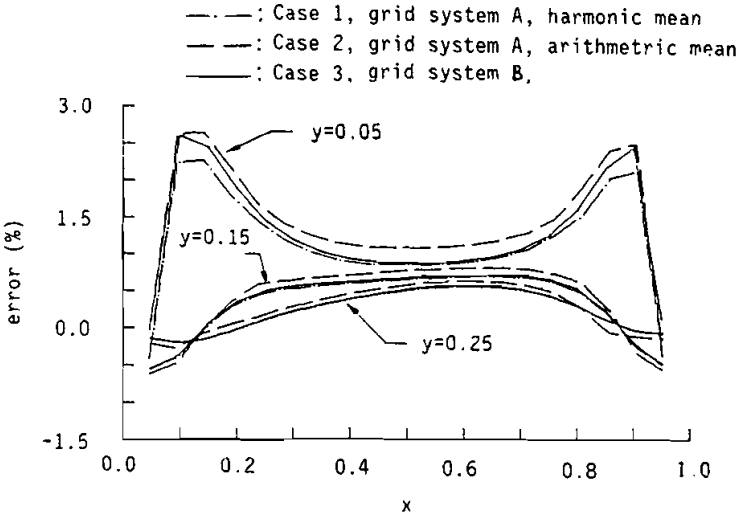

Fig. 4 Comparison of numerical errors generated by cases 1, 2, and 3 at three y positions.

$$T_{i+1/2,j} = \frac{\lambda_2 T_{i+1,j} + \lambda_1 T_{i,j}}{\lambda_1 + \lambda_2} \tag{27}$$

Interpolation of the interface heat flux in grid system B. Since the interface does not coincide with one of the control-volume faces as illustrated in Fig. 3, the interface heat flux should be interpolated from the two heat fluxes at the control-volume faces of grid node (i, j), $q_{i-1/2,j}$ and $q_{i+1/2,j}$, as follows:

$$q_{i,j} = \frac{q_{i-1/2,j} + q_{i+1/2,j}}{2} \tag{28}$$

where

$$q_{i-1/2,j} = -\frac{\lambda_1(T_{i,j} - T_{i-1,j})}{\delta x_{i,j}} \tag{29}$$

$$q_{i+1/2,j} = -\frac{\lambda_2(T_{i+1,j} - T_{i,j})}{\delta x_{i+1,j}} \tag{30}$$

Substitution of Eqs. (29) and (30) into Eq. (28) yields

$$q_{i,j} = \frac{\lambda_1\lambda_2}{\lambda_2 f + \lambda_1(1 - f)} \frac{T_{i-1,j} - T_{i+1,j}}{2\,\Delta x_{i,j}} \tag{31}$$

It is interesting to note that the formulation of $q_{i,j}$ is coincident with the harmonic mean concept if $f = 1/2$, while the temperature gradient is calculated from two alternate grid nodes $(i - 1, j)$ and $(i + 1, j)$ located in the two different material constituents.

The comparisons of the prediction errors of the interface temperature and heat fluxes obtained with cases 1 and 3 are summarized in Tables 1 and 2, respectively. Based on these comparisons, the numerical treatment of case 3 generates more accurate predictions of the interface properties than that of case 1. There are two reasons for this observation. First, the harmonic mean formula of Eq. (15*a*) came directly from the one-

Table 1 Comparison of Prediction Errors of Interface Temperatures in Cases 1 and 3

	Error,[a] %	
y	Case 1	Case 3
0.1	0.893	0.394
0.2	0.681	0.246
0.3	0.480	0.110
0.4	0.353	0.027
0.5	0.311	0.001

[a]Defined by Eq. (23).

Table 2 Comparison of Prediction Errors of Interface Heat Fluxes in Cases 1 and 3

	Error,[a] %	
y	Case 1	Case 3
0.1	0.687	0.018
0.2	2.129	0.075
0.3	0.210	0.004
0.4	0.166	0.003
0.5	0.142	0.002

[a]Defined by Eq. (23).

dimensional analysis, while the present problem is two-dimensional. Second, the temperature function is not differentiable with respect to x at the interface according to the specification of Eq. (3*d*); thus, $\partial^2 T/\partial x^2$ is not defined mathematically at the interface. In the numerical treatment of case 1, this nondifferentiable condition is approximated by use of the harmonic mean operation. The numerical treatment of case 3 does not involve these mathematical defects and, consequently, yields more accurate predictions at the interface than case 1.

Test Problem 2: Heat Conduction with Temperature-Dependent Conductivity

The calculation conditions are the same as for test problem 1, except $\alpha_{10} = 6 \times 10^{-4}$ and $\alpha_{20} = 10^{-5}$. In the problem incorporated with the temperature-dependent conductivity, every pair of neighboring control volumes can be imagined, using the discretization concept, as constructed by two constituents that have different conductivities. In other words, there always exists an abrupt change of conductivity in every pair of neighboring control volumes. Two cases are tested for this problem.

Case 4: Grid system B with the harmonic mean conductivity at each control-volume face.

Case 5: Grid system B with the arithmetic mean conductivity at each control-volume face.

The numerical errors, according to the definition of Eq. (23), are calculated for these two cases at two positions, $y = 0.15$ and $y = 0.25$, and are presented in Fig. 5. It can be seen from the comparison shown in Fig. 5 that the evaluation of conductivity at the control-volume face shows more numerical errors from using the arithmetic mean operation than from using the harmonic mean operation.

CONCLUSIONS

Two conclusions can be drawn in this study:

1. For diffusion-dominant transport problems incorporated with finite-number interfaces with abrupt changes of diffusion coefficients, the grid layout must be

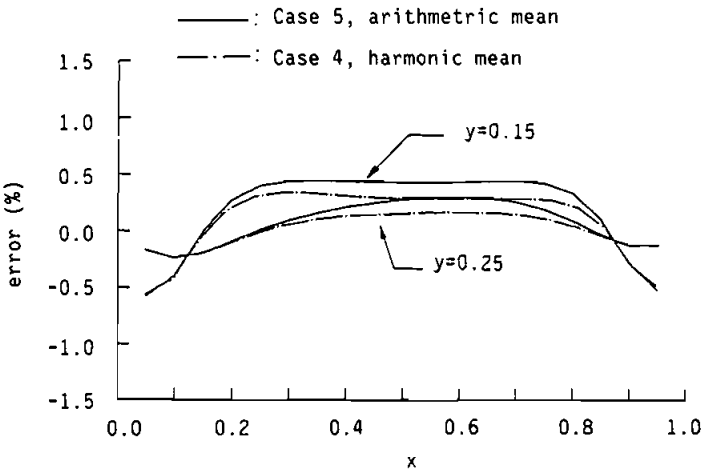

Fig. 5 Comparison of numerical errors generated by cases 4 and 5 at two y positions.

arranged such that each interface with abrupt change of diffusion coefficient is located with a grid node. The formulation of the discretization equations for these control volumes involving the interfaces is straightforward, and no further approximation need be made. This kind of numerical treatment for the interfaces can provide more accurate interface properties.

2. For diffusion-dominant transport problems incorporated with continuous change of diffusion coefficients, the use of the harmonic mean operation in evaluating diffusion coefficients at control-volume faces can yield less numerical error than the use of the arithmetic mean operation does.

REFERENCES

1. S. V. Patankar, *Numerical Heat Transfer and Fluid Flow*, chap. 3, Hemisphere, Washington, D.C., 1980.
2. F. H. Harlow and J. E. Welch, Numerical Calculation of Time-Dependent Viscous Incompressible Flow of Fluid with Free Surface, *Phys. Fluids*, vol. 8, pp. 2182–2189, 1965.
3. S. V. Patankar, A Numerical Method for Conduction in Composite Materials, Flow in Irregular Geometries, and Conjugate Heat Transfer, *Proc. 6th Int. Heat Transfer Conf., Toronto, Canada, 7–11 August 1978*, vol. 3, pp. 297–302, Hemisphere, Washington, D.C., 1978.
4. K. C. Chang and U. J. Payne, Analytical Solution for Heat Conduction in a Two-Material-Layer Slab with Linearly Temperature-Dependent Conductivity, *J. Heat Transfer*, vol. 113, pp. 237–239, 1991.
5. C. Lanczos, *Applied Analysis*, chap. 4, Prentice-Hall, Englewood Cliffs, NJ, 1956.

Received 17 September 1990
Accepted 12 March 1991